Experiments in Fluids 34 (2003) 726–735
DOI 10.1007/s00348-003-0616-y

Corona-induced electrohydrodynamic instabilities in low conducting liquids

F. Vega, A.T. Pérez

Abstract The rose-window electrohydrodynamic (EHD) instability has been observed when a perpendicular field with an additional unipolar ion injection is applied onto a low conducting liquid surface. This instability has a characteristic pattern with cells five to 10 times greater than those observed in volume instabilities caused by unipolar injection. We have used corona discharge from a metallic point to perform some measurements of the rose-window instability in low conducting liquids. The results are compared to the linear theoretical criterion for an ohmic liquid. They confirmed that the minimum voltage for this instability is much lower than that for the interfacial instability in high conducting liquids. This was predicted theoretically in the dependence of the critical voltage as a function of the non-dimensional conductivity. It is shown that in a non-ohmic liquid the rose window appears as a secondary instability after the volume instability.

1 Introduction

The stability of a perpendicular-field fluid interface is a classical problem in electrohydrodynamics. One of the instabilities associated with this problem is the unipolar-injection induced instability. Although corona discharge is a very well-known experimental technique, it has not been applied extensively to produce liquid motion. There is only some descriptive work on the EHD instabilities induced by unipolar charge injection using the corona discharge, such as in the works by Herrick (1974), Ahmed El-Haddad et al. (1980), Malraison and Atten (1991).

Received: 4 February 2002 / Accepted: 9 December 2002
Published online: 14 May 2003

F. Vega (✉), A.T. Pérez
Depto. Electrónica y Electromagnetismo,
Facultad de Física, Universidad de Sevilla,
Avda. Reina Mercedes,
s/n. 41012, Sevilla, Spain
E-mail: fvega@us.es

The authors wish to thank Professor Francisco Pontiga for fruitful discussions and "Taller de la Facultad de Física" of the University of Seville for technical assistance. This work has been carried out with financial support from the Spanish Government (Ministerio de Ciencia y Tecnolog, MCYT) under research project BFM2000-1056

The corona discharge occurs when a gas in the vicinity of an electrode loses its electrical neutrality due to a very high non-homogeneous electric field. A non-homogeneous electric field can be obtained, for example, in a tip–plane configuration. If the DC voltage applied to the tip is high enough (above a certain threshold) the ionisation can sustain a continuous discharge (corona) that produces a stationary space charge distribution. Actually, corona discharge is a rather complex phenomenon (Hish and Oskam 1978), depending on many physical and geometrical parameters. However, for the problem to be treated in this work, the EHD instability at a two-fluid interface, the corona discharge is used merely as a continuous source of ions, and the detailed processes involved in the discharge do not have any significant influence.

Corona discharge provides a technique to reproduce experimentally the EHD instabilities in liquids under a perpendicular field and steady unipolar charge injection that appear in the theoretical models developed in the works by Atten and Moreau (1972), Lacroix et al. (1975), Atten and Lacroix (1979), Schneider and Watson (1970), Koulova-Nenova and Atten (1997), Koulova-Nenova and Atten (1998), Atten and Koulova-Nenova (1999) and Vega and Pérez (2002). In these works the non-ohmic conduction is supposed to be a consequence of the presence of a space charge source (an injecting electrode). Actually, not only injection itself can contribute to the appearance of a space charge in the dielectric fluid. In the case of an insulating liquid other processes due to the existence of a residual conductivity, like recombination and dissociation reactions in the bulk of the fluid, may have an influence and modify the EHD instability criteria (Atten 1975; Pontiga et al. 1995; Pontiga and Castellanos 2000). This residual conductivity could be one of the reasons for the disagreement between theory and experiments, and, consequently, some effort has been done experimentally to eliminate its effect (Lacroix et al. 1975; Atten and Lacroix 1979). However, it seems that the disagreement comes from the difficulty of reproducing exactly in an experimental set-up all the theoretical assumptions made in the resolution of the problem of unipolar injection. For a general review and references of the unipolar injection problem in electrohydrodynamics, see Castellanos et al. (1998).

In this work, we study experimentally the electrohydrodynamic instabilities induced by corona discharge in very low conducting liquids. First of all, as the ion density in air is low enough (n_0~400 cm^{-3}) the residual conductivity C_0 (Pontiga and Castellanos 2000) is small and the

effects of recombination reactions can be neglected: $C_0=en_0L^2/(\varepsilon_0 V)\sim 5\cdot 10^{-10}\ll 1$, where L is the air layer thickness and V the applied electric potential (around 1 to 10 kV in the measurements). We consider two different cases: liquids in ohmic and non-ohmic regimes. In both cases the liquid layer is in contact with the air, and the air is in contact with the injecting electrode. When a charge injection is exerted into the air layer the electric field pushes down the space charge towards the interface. If the liquid is in non-ohmic regime this space charge penetrates through the interface and induces electric forces in bulk of the liquid that can produce the classic EHD convective instability. This instability has a characteristic wavelength of the order of the liquid layer thickness (Atten and Moreau 1972). Lacroix et al. (1975) and Atten and Lacroix (1979) studied the convective instability in an experimental set-up where the ions are directly injected into an insulating liquid layer with the use of an electrodialytic membrane that serves as a rigid injecting electrode (Felici and Tobazeon 1981). Watson et al. (1970) reproduced this instability experimentally with the use of an electron beam that injects space charge into an insulating liquid layer in a vacuum. The theoretical model that closely approaches this experiment can be found in the work by Schneider and Watson (1970). The injecting electrode here is the liquid free surface. The electron-beam charge injection technique is described by Watson and Clancy (1965). The corona discharge from a tip produces the same convective instability in very low conducting liquids as was demonstrated by Malraison and Atten (1991). We have reproduced this experiment and some of the resulting measurements concerning this instability are presented here.

But another possible and much less known instability in a perpendicular-field unipolar injection problem is the rose-window instability, which is a phenomenon that until now has been observed only in low conducting liquids in contact with air (Pérez 1997) and subjected to corona discharge. Other authors (Herrick 1974; Ahmed El-Haddad et al. 1980) have observed similar patterns, but their descriptions do not help to clarify under what experimental conditions and in what kind of liquids they are observable. A theoretical description of the instability mechanism in the case of an ohmic liquid was carried out by Vega and Pérez (2002). It is clear that in the air the effects of a residual conductivity are negligible and in this theoretical analysis they have not been taken into account. Under unipolar charge injection and provided the liquid conductivity is low enough an electric pressure of the same sign of the applied electric field is exerted onto the interface. This electric pressure can produce a surface deformation above a certain threshold. The perturbation is kept because the current density (and, correspondingly, the electric pressure) is higher in the thinner areas of the deformed interface (Vega and Pérez 1999b). The deformation has a characteristic wavelength typically about five to 10 times larger than in the convective instability. Therefore the rose-window instability can be grouped into the type of interfacial instabilities, like those in an ohmic/ohmic interface (Melcher 1963; Melcher and Smith 1969; Chu et al. 1989; Néron de Surgy et al. 1993; González et al. 1994; Néron de Surgy 1995; El-Dib 1999), as they are due to the destabilising effect of the electric pressure over the fluid interface, but unlike the cases considered by these authors, it is characterised by the existence of a space charge distribution in one or both sides of the interface. We present here a set of measurements for the rose-window instability. We think they are strong experimental evidence of one of the possible interfacial EHD instability mechanisms in a perpendicular-field non-ohmic/ohmic interface (Vega and Pérez 2002). The measurements we performed also provide evidence that corona discharge is a valid experimental technique for obtaining the rose-window and the convective EHD instabilities in air/liquid interfaces.

The two experimental set-ups that are used in this work are described in Sect. 2. With one of the experimental set-ups we have tried to approach the plane geometry model in order to compare the experimental results with the theory. In Sect. 3 the results are presented, together with a set of photographs of the instabilities. A comparison with theory (Vega and Pérez 2002) is provided in Sect. 4. Finally we present our conclusions in Sect. 5.

2 Experimental set-up

In the experimental set-up we place a metallic tip (tungsten) of about 10 μm radius above the centre of a circular plane electrode of 4.5 cm diameter. The electrode is a transparent glass with a thin conducting coating. The liquid is placed over this plane electrode. A mirror below the transparent electrode is used to deviate the image of the liquid surface to a camera system that amplifies it to detect the deformation. A ring of acrylic glass prevents the leakage of the liquid (see Fig. 1a). This acrylic glass support is fixed onto a table (Melles Griot model, Voisins Le Bretonneux, France) through an acrylic glass structure of 15 cm height (Fig. 1b). The electrode is connected to an electrometer (model 6512, Keithley Instruments, Cleveland, Ohio, USA) in order to measure the electric current through the liquid. The tip is connected to a high voltage source (model RHR40PN120/OV/FG, Spellman High Voltage Electronics, Hauppauge, N.Y., USA). The ions from the corona discharge reach the plane electrode by electric repulsion from the tip and exert an electric pressure over the liquid. This is called the "tip–plane set-up". The hyperbolic geometry of the electric field in a tip–plane configuration (Coelho and Debeau 1971) makes it difficult to compare with the plane geometry models used in a theoretical analysis of the problem. Besides, the space charge distribution caused by corona discharge in a tip–plane configuration is far from homogeneous (Atten 1996; Giacometti 1987). This is why a metallic grid can be optionally interposed between the tip and the circular electrode. The grid we used is square-shaped with copper wires of a=0.25 mm diameter and a separation of b=1.5 mm between the wire centres. This grid is connected to another high voltage source (model 610C, Trek Inc., Medina, N.Y., USA), which provides a more homogeneous electric field and corona distribution over the liquid surface. The electrode is required to be transparent in order

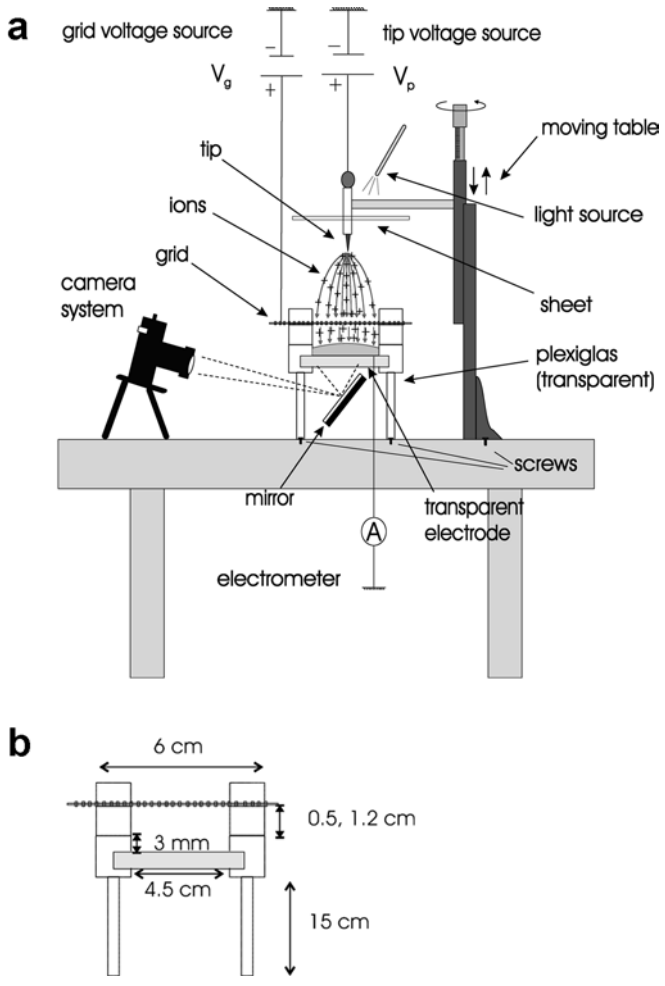

Fig. 1. **a** Scheme of the triode set-up. The tip-to-plane distance is p and the grid-to-plane distance is h. **b** The dimensions of the grid–plane system

to have a clear image from below if the metallic grid is used. The complete set-up, called "triode" (three-electrode system) is shown in Fig. 1b. The grid is held between two other acrylic glass rings that are screwed to the first one, and then the set of acrylic glass rings, transparent electrode and grid are firmly fixed. We can also vary both the tip–plane distance, as the tip is held by a metallic rod fixed perpendicularly to a moving plane, and the grid–plane distance, as we have a set of acrylic glass rings with different thicknesses. The tip–plane and grid–plane distances are of the order of 1 cm.

Figure 2 is a plot of the current that arrives at the plate as a function of the grid voltage for different tip voltages, in the absence of liquid. When the grid voltage is zero, no current reaches the plane electrode. (Actually, there is a current caused by corona wind, see the work by Giacometti and Sinézio (1990), but it is too small to produce instability.) If we raise the grid voltage the current grows and, at the same time, the electric field over the liquid is higher. When the grid voltage is high enough to decrease the corona current coming from the tip, the current into the liquid starts to decrease. With the tip–grid–plane configuration it is possible to apply to the liquid the same electric field with different electric currents, by varying the tip voltage.

We have used extensively three liquids. Under our experimental conditions and because of their initial conductivities, two of the liquids are in the ohmic regime (castor and corn oils) and the third one is in the non-ohmic regime (silicone oil). The properties of the liquids are represented in Table 1. These properties have been measured in our laboratory. Specifically, the conductivity has been measured with a conductivity meter IRLAB model LDTRP-2. We have performed measurements with several volumes of liquid to vary the liquid layer thickness that is typically of the order of 1 mm. All measurements were performed in Seville, Spain, April–May (Figs. 3, 5, 9, 10, 11, 12, 13, 14, 15, 16) and November (Figs. 4, 6, 7 and Table 2) 2001.

Table 1. Physical properties of the liquids used in the experiments, ε is the relative electric permittivity and ν is the kinematic viscosity

Oil	ε	ρ (kg/m^3)	ν (m^2/s)	K(m^2/Vs)	σ (Ω^{-1}m^{-1})
Silicone	2.73	960	$50{\cdot}10^{-6}$	$5{\cdot}10^{-10}$	$6{\cdot}10^{-13}$
Castor	4.69	958	$600{\cdot}10^{-6}$	$4{\cdot}10^{-11}$	$7{\cdot}10^{-11}$
Corn	3.1	990	$55{\cdot}10^{-6}$	$4.5{\cdot}10^{-10}$	$1.9{\cdot}10^{-11}$

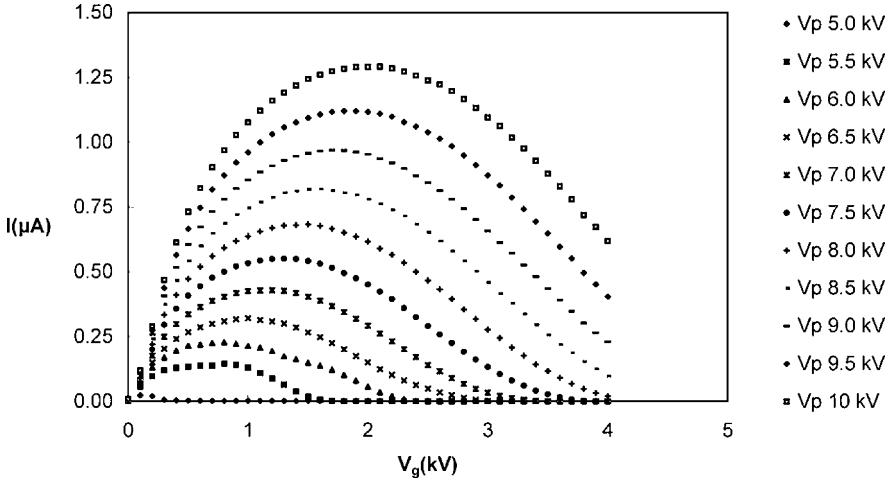

Fig. 2. Electric current I that arrives at the plate as a function of the grid voltage V_g (triode set-up) for different tip voltages V_p. Distances are: between the tip and the grid $p-h$=3.0 cm, and between the grid and the plate h=0.5 cm. The electrode area in this series is $A=1.96{\cdot}10^{-3}$m^2

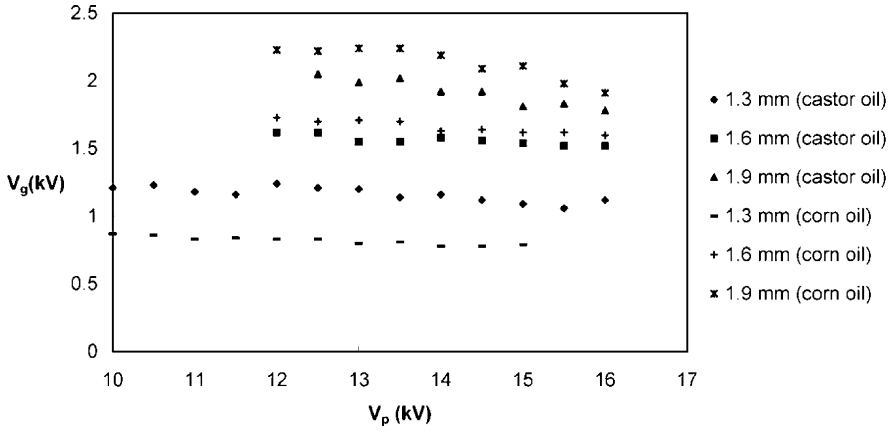

Fig. 3. Rose-window instability. Critical grid voltages for liquids in the ohmic regime (castor oil and corn oil) as a function of the tip voltage in a triode set-up, for several liquid layer thicknesses. Distances are: $p-h$=2.5 cm, h=1.5 cm. In all measurements, the electrode area is $A=1.59\cdot10^{-3}$ m^2 (diameter: 4.5 cm)

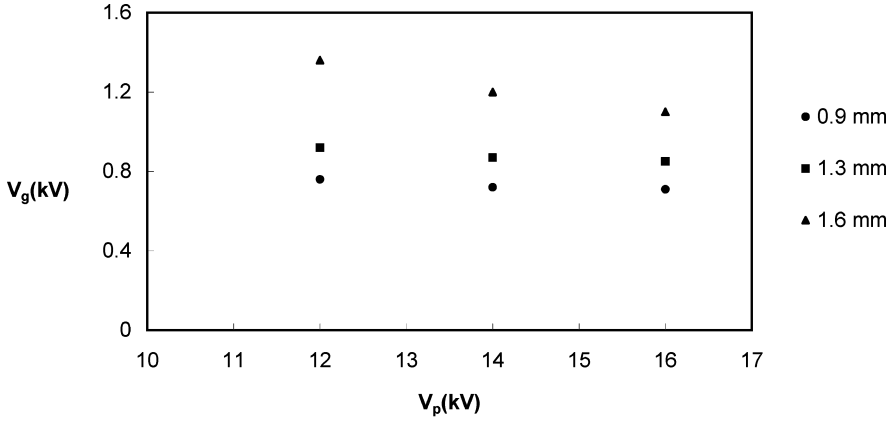

Fig. 4. Rose-window instability. Critical grid voltages as a function of the tip voltage in a triode set-up, for several liquid layer thicknesses. Liquid: silicone oil (non-ohmic). Distances are: $p-h$=2.5 cm, h=0.8 cm

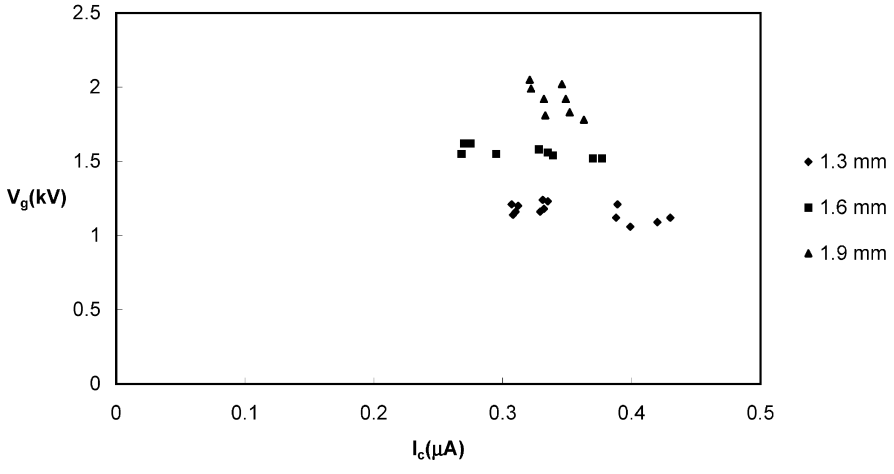

Fig. 5. Rose-window instability. Critical grid voltages as a function of the electric current in a triode set-up, for several liquid layer thicknesses. Liquid: castor oil (ohmic). Distances are: $p-h$=2.5 cm, h=1.5 cm

Table 2. Critical values of the current density in silicone oil (non-ohmic behaviour). Triode set-up. Tip–grid distance: 3.5 cm, grid–plane distance: 0.8 cm

d(mm)	I(μA)	$I(A)d^3$ (m)
0.13	0.262	$6.45\cdot10^{-19}$
0.18	0.108	$6.31\cdot10^{-19}$
0.22	0.058	$6.61\cdot10^{-19}$
0.27	0.003	$6.50\cdot10^{-19}$
0.31	0.020	$6.25\cdot10^{-19}$
0.36	0.013	$6.07\cdot10^{-19}$
0.40	0.010	$6.31\cdot10^{-19}$
0.45	0.007	$6.31\cdot10^{-19}$

2.1 Measurements

The critical points were obtained by taking the voltage at the first surface deformation. The deformation was observed through a photographic objective. We have noted that the use of transparent electrodes makes visual observation equally as sensitive for detecting the instability as other methods that we have designed (see, for example, the work by Pérez (1997)). In the tip–plane set-up the tip voltage is raised until the instability starts. This value of the tip voltage is taken as the critical value. The liquid used in this set-up must be viscous enough to avoid

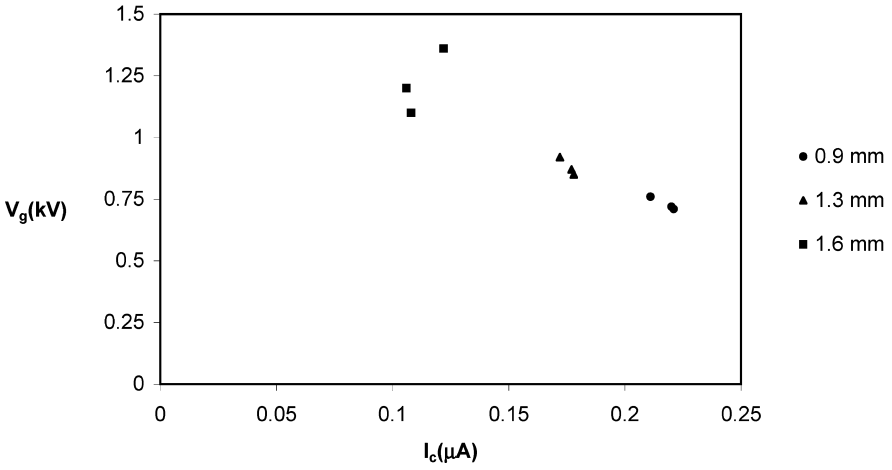

Fig. 6. Rose-window instability. Critical grid voltages as a function of the electric current in a triode set-up, for several liquid layer thicknesses. Liquid: silicone oil (non-ohmic). Distances are: $p-h$=2.5 cm, h=1.5 cm

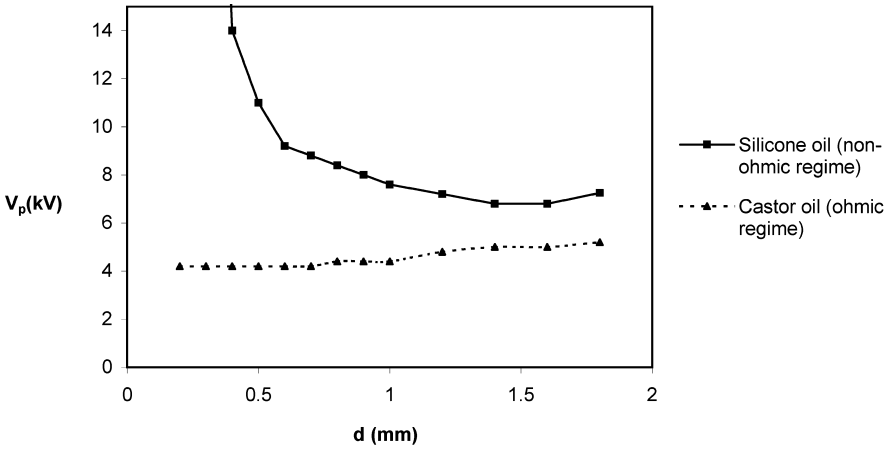

Fig. 7. Rose-window instability for very thin liquid layers in an ohmic liquid (castor oil) and in a non-ohmic liquid (silicone oil). In this plot V_c is the tip voltage at which the instability is first observed, and d is the liquid layer thickness. In the case of castor oil the instability is observed as soon as the corona threshold is reached. Tip-to-plane distance p=3.0 cm

the effects of the corona wind: if the viscosity is low, the surface of the liquid moves too much before the instability onset and it is not possible to study the instability from an initial static state. Some tests have been performed in low viscous liquids, like water, and the effect of the corona wind is to disturb the liquid surface, just below the tip centre. In the case of the triode set-up (Vega and Pérez 1999a), the corona wind is largely suppressed by the grid. To take the critical points in the triode we fix the tip voltage and vary the grid voltage. The critical grid voltage is taken when the first surface deformation occurs, which happens always when the current is increasing with the grid voltage, if the tip voltage is high enough. The grid voltage controls, essentially, the electric field onto the liquid surface.

The critical voltages for the rose-window instability in a triode set-up are shown in Figs. 3 and 4 for the three different liquids. These critical grid voltages are plotted as a function of the tip–plane voltage. The critical voltages show a clear tendency to increase for thicker liquid layers. Also the critical grid voltages show a tendency to decrease with the tip voltage. This is a consequence of the fact that the current density reaching the liquid increases with the tip voltage. Then the electric pressure for equal grid voltages increases with the tip voltage. This is in agreement with the tendencies shown in Figs. 5 and 6, where the critical grid voltages are plotted against the electric current. Although the dispersion of the electric current data is high because the current value is very sensitive to a grid voltage variation (a rough estimation from the experimental current curves shows that a typical error in the grid voltage of 50 V induces an error of about 0.025 μA in the current), it can be seen that the critical electric current decreases if the critical voltage increases. In the non-ohmic liquid it is also clear that the critical current increases if the liquid thickness decreases, which is not so evident in the ohmic liquid.

In the case of a non-ohmic liquid, there are two critical values corresponding to the two possible instabilities: the convective instability and the rose-window instability. Among the three liquids used we have only seen convective instability in silicone oil, providing in this case evidence of the existence of space charge in the volume of the liquid. The conduction regime of the liquid can be estimated as follows: the characteristic non-ohmic conduction time in silicone oil layer with d=1 mm (see properties in Table 1) is $d^2/K_1V_1 \sim 10^{-6}/(5\cdot10^{-10}\cdot2\cdot10^2) \sim 10$ s (being V_1 the voltage drop through the liquid layer and K_1 the ion mobility in the liquid) and the charge relaxation time is higher: $\varepsilon_1/\sigma = 2.73\cdot8.85\cdot10^{-12}/(6\cdot10^{-13}) = 40$ s (ε_1 is the dielectric constant in the liquid) and then there is a net space charge in the bulk of the layer (besides, in this work d<2 mm). A similar estimation in castor and corn oil gives charge relaxation times lower than the non-ohmic con-

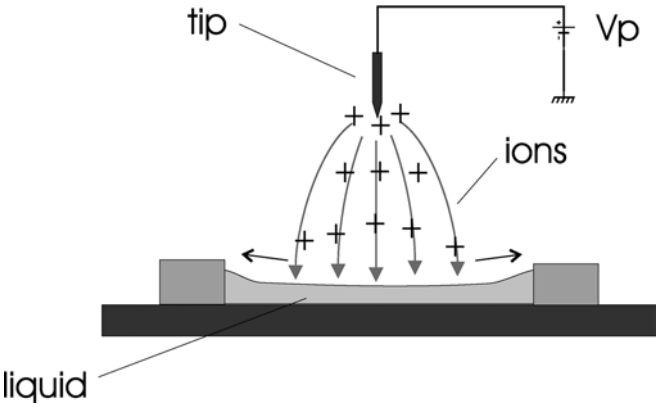

Fig. 8. The electric pressure pushes down the liquid, curving the liquid surface

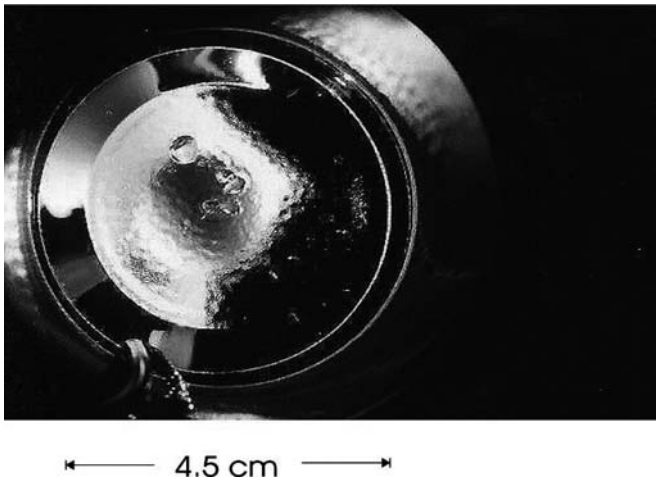

Fig. 9. Convective instability (image from below). Tip–plane set-up. Liquid: silicone oil. V_p=8.2 kV, p=3.0 cm, d=1.2 mm

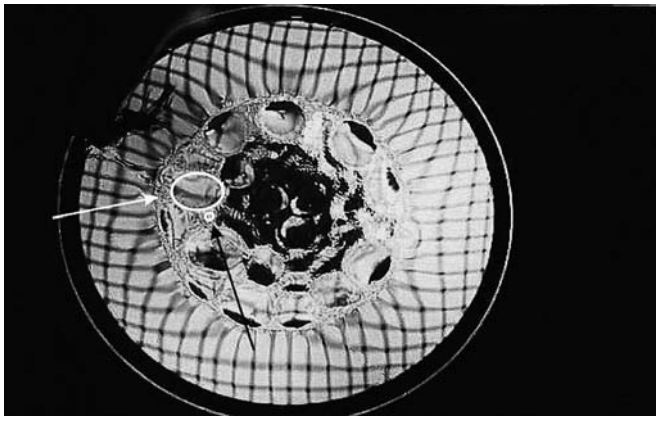

Fig. 10. Coexisting instabilities (convective and rose window) in a non-ohmic liquid (silicone oil). Typical cells of the convective and of the rose-window instabilities are indicatedby *black* and *white arrows*, respectively. It can be seen that the cell size of the convective instability is comparatively much smaller. A small rugose pattern appears in the image that is produced by the convective instability in the liquid surface. Triode set-up. V_p=12 kV, V_g=3.0 kV, I=1.0 μA, d=1.2 mm, p=3.0 cm, h=1.5 cm

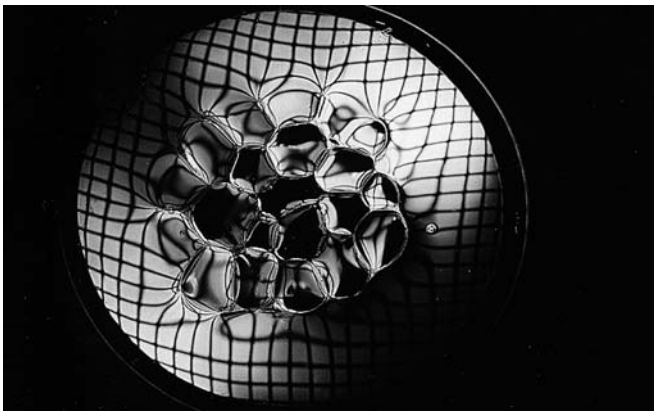

Fig. 11. Rose-window instability in an ohmic liquid (castor oil). The small wavelength instability is absent. V_p=8.8 kV, V_g=2.0 kV, I=0.63 μA, d=1.2 mm, p=3.0 cm, h=1.5 cm

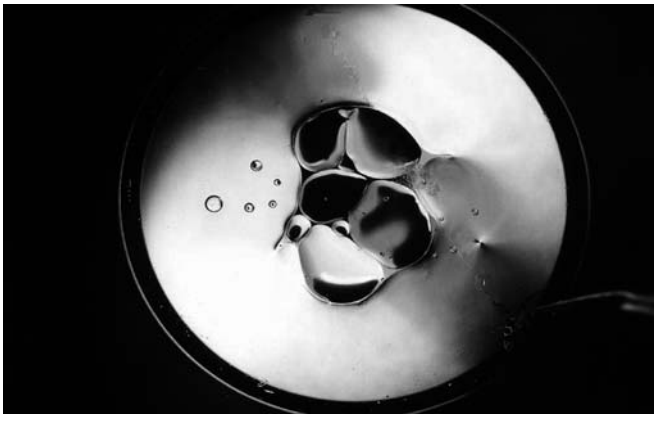

Fig. 12. The non-homogeneity of the electric field is greater in a tip–plane configuration. The first incipient instability appears at the centre of the electrode. Liquid: castor oil. V_p=6.8 kV, I=0.404 μA, L=3.1 cm, p=3.0 cm, d=1.2 mm

duction characteristic time, which means that the electric conduction is ohmic, and no space charge can be supported.

Theoretically, the behaviour of the rose-window instability for small liquid thicknesses is expected to be very different in ohmic and non-ohmic liquids: while in ohmic liquids the critical voltage tends to a small value, in non-ohmic liquids it tends to infinity near a critical value d^{crit} and down to this value the instability is absent. Then, the two types of conduction regimes are supposed to have an opposite behaviour for very thin liquid layers. This behaviour is found experimentally as shown in Fig. 7 where critical values for thin liquid layers in a tip–plane set-up have been plotted for silicone oil (non-ohmic) and castor oil (ohmic). Note that the tip critical voltage is plotted in the vertical axes in this figure. In this set-up there is no current below the corona threshold and a fortiori the critical voltages are always greater than the corona threshold.

In Table 2 we present the results for the convective instability in the non-ohmic liquid in the tip–plane and the triode configurations. As we see the magnitude $I{\cdot}d^3$ is

Fig. 13. Rose window fully developed in an ohmic liquid (castor oil) in a triode set-up. The instability is stationary even at voltages higher than the critical value. V_p=12 kV, V_g=3.25 kV, I=1.55 μA, p=3.0 cm, h=1.5 cm, d=1.2 mm

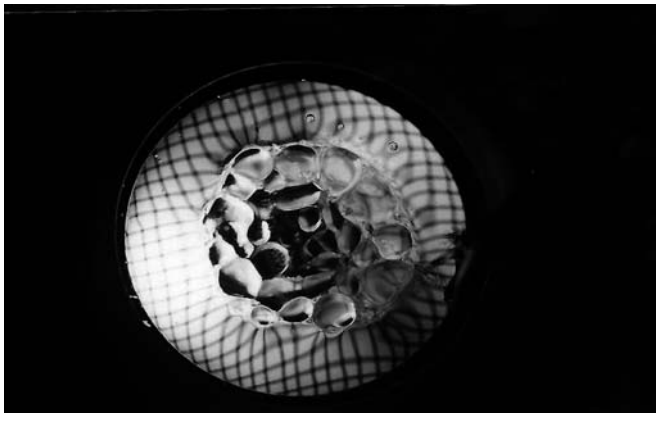

Fig. 14. Rose-window instability in corn oil in a triode set-up. There is not a noticeable difference in the characteristic pattern for different ohmic liquids (compare with Fig. 11). V_p=9.0 kV, V_g=2.8 kV, I=0.612 μA, p=3.0 cm, h=1.5 cm, d=1.2 mm

Fig. 15. Deformations at the centre of each grid square in the decreasing region of the corona current in a triode set-up. Liquid: castor oil. V_p=10 kV, V_g=5.0 kV, I=0.713 μA, p=3.0 cm, h=1.5 cm, d=1.2 mm

approximately constant. This can be explained if we consider that the liquid layer is in the space charge limited current (SCLC) regime: the voltage drop across an insulating liquid layer under strong charge injection is $\sqrt{8jd^3/9K_l\varepsilon_l}$. Then if $I{\cdot}d^3{\sim}c$, c being a constant, it follows that V_l is also a constant V_l is proportional to $T{=}\varepsilon_l V_l/K_l\eta$, which is the characteristic parameter of the instability criterion for an insulating liquid layer subjected to unipolar injection (where η is the dynamic viscosity). These results are quite similar to those in the work by Malraison and Atten (1991), where the experimental values are higher than the theoretical ones: Schneider and Watson (1970) predict $I{\cdot}d^3{=}2.88{\cdot}10^{-19}$ Am^3 for the critical current, while we obtained an average value $I{\cdot}d^3{\sim}6.35{\cdot}10^{-19}$ Am^3, which corresponds to $T_c{\sim}250$. This difference could be due to a lower effective liquid layer thickness, as the liquid is pushed down by the corona wind (Fig. 8). Nevertheless, an agreement of our experimental measurements with the theory (Schneider and Watson 1970; Koulova-Nenova and Atten 1997) could not be expected as the experimental conditions in both set-ups are quite different to those in the theory. (For example, the theory assumes that the liquid surface is equipotential which is not necessarily true in our experiments.) Besides, because of its small wavelength (less than 1 mm), this instability is difficult to detect visually and the measured values could not be but an upper bound for the critical voltage. It is also interesting to note that in other experimental configurations the change of slope in the current vs. voltage curve is the best way to detect the instability, but this change of slope is not accessible in our experimental set-up because we cannot measure the voltage of the liquid surface (Lacroix et al. 1975).

2.2 Photographs

By use of a camera we can amplify the image of the liquid surface as seen from below. This is possible because of the transparency of the plane electrode and the liquids. Figure 9 shows the convective instability in a tip–plane set-up, with a small characteristic wavelength. The liquid is silicone oil. Noticeable also is a first deformation with a much longer wavelength (5–10 mm), which is the rose-window instability. This long wave instability has another important characteristic, which is a typical higher deformation amplitude and this makes it easier to be detected. In a non-ohmic liquid the rose window is a secondary instability because, in general, it appears once the convective instability has already developed. Since the convective instability is absent in liquids in the ohmic regime, its detection is also an experimental criterion for checking out the type of conduction regime of a liquid.

In Figs. 10 and 11 the rose-window instability is shown for silicone and castor oil, respectively, in a triode set-up. Both instabilities coexist in the non-ohmic liquid whereas the convective instability is absent in the ohmic liquid. It should be mentioned that the rose-window instability does not develop abruptly but gradually. A first stationary deformation of high amplitude is detected at a given potential. This deformation appears at the centre of the electrode because the electric field there is more intense owing to its non-homogeneity. This effect is stronger in a tip–plane configuration, where this inhomogeneity is more important. Figure 12 shows that close

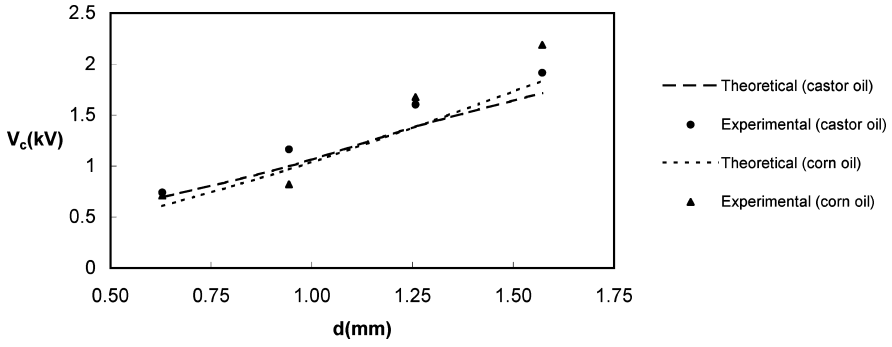

Fig. 16. Rose-window instability. Comparison between theoretical and experimental critical voltages for the ohmic regime. The experimental series correspond to the triode set-up, with $p-h$=2.5 cm, h=1.5 cm. The critical grid voltage is plotted against the liquid layer thickness

to the instability threshold the deformation is only visible at the centre. If the electric potential is raised, the instability begins to develop over all the electrode area. This transition is shown in Fig. 11 where the rose-window instability is in an intermediate stage of development and in Fig. 13 where the instability has fully developed at a still higher electric potential (around 3 kV). We have observed that the pattern of the rose-window instability is similar for different liquids. For instance, Fig. 14 corresponds to corn oil.

For high grid voltages, when the electric current starts to decrease (see Fig. 2), a rectangular pattern with centred deformations at each rectangle becomes visible (see Fig. 15). This additional pattern may be related to the concentration of the electric field lines in the centre of the grid squares and the corresponding electric pressure distribution onto the liquid surface.

3
Rose-window instability: discussion

In a former work (Vega and Pérez 2002), we have computed the linear instability criterion of the rose-window instability in a perpendicular-field air/ohmic liquid interface. We used a standard treatment of the problem: a small perturbation is introduced in the electrohydrodynamic set of equations and the compatibility condition yields the characteristic eigenvalue in the dispersion relation. In this problem the eigenvalue is $U=\varepsilon_0 V^2/<\rho>gh^3$, indicating that the equilibrium between electric and gravitational pressure rules in the instability onset. The dispersion relation $U(k)$, where k is the non-dimensional wave number, is also a function of other magnitudes:

$$U(k,\ Bo,\ C,\ S,\ \varepsilon,\ d^*) \tag{1}$$

where all these magnitudes are non-dimensional:

$$Bo=\frac{<\rho>gh^2}{\gamma}\ ,\quad C=\frac{q_0 h^2}{\varepsilon_0 V}\ ,\quad S=\frac{\sigma h^2}{K_a \varepsilon_0 V} \tag{2}$$

$$\varepsilon=\varepsilon_l/\varepsilon_0,\quad d^*=d/h \tag{3}$$

where $<\rho>$ is the mass density jump at the interface, g the gravitational acceleration, h is the total length of the system $h=L+d$, L and d being the air and the liquid layer thickness, respectively. The parameter Bo is the Bond number, which is a relation between the gravitational and capillary forces, C is the injection parameter that measures the strength of the injection and q_0 is the space charge density at the injecting electrode. We refer to S as the apparent conductivity. It is a relation between the magnitudes of the non-ohmic and ohmic current densities in a non-ohmic layer with ion mobility K_a and an ohmic layer with conductivity σ. The apparent conductivity controls the interfacial instability mechanism in a non-ohmic/ohmic fluid interface.

If the non-dimensional conductivity S is high enough the instability that first appears is normally the classical interfacial instability, which has an electric pressure directed upwards. If this is the case, the critical voltages for a system with characteristic lengths of the order of 1 cm for the air layer and 1 mm for the liquid layer are of the order of 50–100 kV. These critical values are of the order of those for the interfacial EHD instability in conducting liquids in the case of no injection. Conversely, if the non-dimensional conductivity S is low enough the instability that first appears is the rose-window instability, as the electric pressure is directed downwards, with critical values around 1 kV. The typical values of the magnitudes we deal with in our experiments ($K_a \sim 10^{-4}$ m^2/(Vs), $h\sim 10^{-2}$ m, $<\rho>\sim 10^3$ kg/m^3) and the conductivity of the liquids we used are compatible with the occurrence of the rose-window instability.

Concerning the injection level, Vega and Pérez (2002) found theoretically that the critical voltage for instability for low S is a strongly decreasing function of the parameter C in the weak injection region. Once the SCLC regime (strong injection) is reached the eigenvalue becomes independent of C. All this is concordant with our experimental observations. Below the corona onset there is no instability if no charge injection is applied. If a strong charge injection (a tip potential higher than the corona threshold) is applied, the critical values observed in the triode set-up are of the order of 1 kV, as expected theoretically. The critical points of Figs. 3 and 4 show a weak dependence on the tip voltage (that controls the space charge in the triode system). This agrees with the fact that in the range of $V_g\sim 1$ kV and $V_p\sim 10$ kV the electric current increase with the tip voltage tends to be weak (see Fig. 2).

Figure 16 compares the critical values of the electric potential obtained theoretically and experimentally (in ohmic regime). They agree in order of magnitude and show the same tendency. The theoretical values are calculated according to the linear model (Vega and Pérez 2002). They were obtained in the strong injection limit and neglecting the effects of capillary forces. The experimental critical values of the electric current I_c (Figs. 5 and 6) are

also in the range of those predicted by the theory (of the order of 0.1–1 μA).

Of specially interest is the dependence of the critical voltage on the liquid layer thickness. As we saw in subsection 1, the rose window in very thin layers appears only in the ohmic case. This experimental evidence agrees with the theory and it can be explained because in non-ohmic liquids the electric pressure over the surface is an increasing function of the thickness if the liquid layer is thin enough. Therefore the interfacial instability for a low conducting liquid is not possible below a critical thickness $d^{\star}<d^{\star\mathrm{crit}}$ (Atten and Koulova-Nenova 1996). Conversely, in ohmic liquids, and for low values of S, the electric pressure jump always increases if the relative thickness $d^{\star}$ decreases, and consequently the instability is possible for all $d^{\star}$ values (Vega and Pérez 2002). The experimental value is $d^{\star\mathrm{crit}}\sim 0.011$, while an estimation of the value by Atten and Koulova-Nenova (1996) is $d^{\star\mathrm{crit}}\sim 0.015$ for silicone oil. In consequence, the absence of the rose-window instability in a thin layer proves that the liquid is in the non-ohmic regime and conversely, the appearance of the rose-window instability in a thin layer proves that the liquid is in the ohmic regime and that the convective instability caused by charge injection will not appear.

Another important point is the fact that the rose-window instability does not grow violently above the critical value V_c. This is in contrast with the case of conducting liquids with no injection (Néron de Surgy et al. 1993; Néron de Surgy 1995; Melcher and Smith 1969), where the surface deforms abruptly and the liquid eventually reaches the opposite electrode, producing a short circuit. This proves experimentally that in the rose window the electric pressure is not directed upwards, and its dynamics defer from that in an ohmic–ohmic interface (for the study of an ohmic–ohmic interface, see Melcher and Smith (1969), Melcher and Taylor (1969), and Melcher and Schwarz (1968)).

With respect to the behaviour of the rose-window instability in non-ohmic liquids, there is not a precise theoretical model yet. The difficulty is that in those liquids the rose window is a secondary instability (and this has been shown clearly in our experiments) that appears after the classical convective instability caused by unipolar injection. In this case a linear treatment from an initial static state is not possible. Nevertheless, it is clear that the instability appears in the same range of critical potentials. The secondary rose-window instability was not observed by Malraison and Atten (1991), where the same non-ohmic liquid was used (silicone oil), because the distance between the injecting electrode and the liquid surface was too high, showing again that the critical parameter is related to the mean electric field $E_0=V/h$ through
$U = \varepsilon_0 E_0^2/ < \rho > gh.$

4
Conclusions

In this work we have used corona discharge in air to produce unipolar-injection induced electrohydrodynamic instabilities. Two experimental set-ups have been studied: a tip–plane configuration and a triode set-up. The triode set-up is intended for correcting the non-homogeneity of the electric field in order to reproduce better theoretical models of plane geometry. The measurements were performed in low conducting liquids in ohmic and non-ohmic regimes.

In the case of a non-ohmic regime we have also observed the classical convective instability in insulating liquids subjected to unipolar injection. We have seen that this instability does not appear in more conducting liquids (in the ohmic regime), confirming that this instability is due to electric bulk forces. The rose-window instability has been proved to be a secondary instability in the case of a liquid in the non-ohmic regime, in the sense that we have observed it always after the convective instability and coexisting with it. The question arises whether both instabilities could exist independently or if they are interconnected. We think, since the scales are quite different, that it should be possible to describe the rose-window instability in non-ohmic liquids alone, making some average over the fluid velocities and space charge distribution of the already disturbed liquid layer, but no attempts have been made in this direction yet.

In the ohmic regime, a reasonable quantitative agreement has been found between the experimental behaviour (in a triode set-up) of the rose-window instability and the theory (Vega and Pérez 2002). The behaviour with conductivity, dielectric constant, liquid layer thickness and injection level is compatible with that model. Another important characteristic predicted theoretically (Vega and Pérez 2002; Atten and Koulova-Nenova 1996) has been verified: the behaviour of the rose window with the liquid layer thickness is opposite in the ohmic and non-ohmic regimes for very thin liquid layers. While in non-ohmic regimes the instability critical voltages tend to infinity if $d^{\star}<d^{\star\mathrm{crit}}$, in ohmic regimes they tend to low values.

In spite of the differences between the experimental conditions and the theoretical assumptions, it is clear that the rose-window instability is a long-wave instability that is possible because there exists a space charge distribution impinging on the surface. This space charge, originated by the corona discharge in our experiments, reduces the critical voltage by more than an order of magnitude if we compare it with the critical voltage needed to destabilise a conducting liquid surface.

For future works, the experimental set-up must be greatly improved in order to assure a good convergence with the theoretical model in all ranges of conductivity and the other parameters (this first study has been limited to the range of low conductivity).

References

Ahmed El-Haddad AT, Fornazéro J, Mesnard G (1980) Mécanismes de base de la déformation cellulaire d'une couche mince isolante liquide soumise à un flux de charges. Phys Chem Liq 9:201–218

Atten P (1975) Stabilité des liquides de faible conductivité. J Mécan 14:461–495

Atten P (1996) On the use of an ionic pump in a convector heater. IEEE Trans Ind Appl 32:80–89

Atten P, Koulova–Nenova D (1996) EHD instability of insulating liquids due to charge injection from the free surface. In: Confer-

ence Record of the Twelfth International Conference on Dielectric Liquids (ICDL '96), Roma, Italy. IEEE Dielectrics and Electrical Insulation Society, pp 476–479
Atten P, Koulova-Nenova D (1999) On the instability between two layers of conducting and insulating liquids subjected to a DC field. In: Proceedings of Thirteenth International Conference on Dielectric Liquids (ICDL '99), Nara, Japan. IEEE Dielectrics and Electrical Insulation Society, pp 277–280
Atten P, Lacroix JC (1979) Non-linear hydrodynamic stability of liquids subjected to unipolar injection. J Mécan 38:469–510
Atten P, Moreau R (1972) Stabilité électrohydrodynamique des liquides isolants soumis à une injection unipolaire. J Mécan 11:471–520
Castellanos A, Zhakin AI, Watson PK, Atten P, Chang JS (1998) Electrohydrodynamics. Springer-Verlag, Berlin Heidelberg New-York
Chu XL, Velarde MG, Castellanos A (1989) Dissipative hydrodynamic oscillators. III: Electrohydrodynamic interfacial waves. Il. Nuovo Cimento 11D:727–737
Coelho R, Debeau J (1971) Properties of the tip–plane configuration. J Phys D: Appl Phys 4:1266–1280
El-Dib YO (1999) Nonlinear stability of an electrified interface supporting surface charges between two viscous fluids. J Colloid Interface Sci 210:103–117
Felici NJ, Tobazeon RE (1981) Charge carrier elimination and production by electrodyalitic polymers in contact with dielectric liquids. J Electrost 11:135–161
Giacometti JA (1987) Radial current–density distributions and sample charge uniformity in a corona triode. J Phys D: Appl Phys 20:675–683
Giacometti JA, Sinézio J (1990) Constant current corona triode with grid voltage control. Application to polymer foil charging. Rev Sci Instrum 61:1143–1150
González H, Néron de Surgy G, Chabrerie JP (1994) Influence of bounded geometry on electrocapillary instability. Phys Rev B 50:2520–2528
Herrick CS (1974) Electroconvection cells in dielectric liquids interfaced with conducting fluids. Proc Roy Soc Lond A 336:487–494
Hish MN, Oskam HJ (eds) (1978) Gaseous electronics, vol I. Electrical discharges. Academic Press, New York
Koulova-Nenova D, Atten P (1997) EHD instability of air/liquid two liquid layer system under unipolar charge injection. J Electrost 40/41:179–184
Koulova-Nenova D, Atten P (1998) EHD convective and interfacial instabilities of conducting/insulating two liquid layer system with deformable interface. In: Proceedings of the International Workshop on Electrical Conduction, Convection and Breakdown in Fluids, Universidad de Sevilla. University of Seville, Seville, Spain, pp 65–69
Lacroix JC, Atten P, Hopfinger EJ (1975) Electroconvection in a dielectric liquid layer subjected to unipolar injection. J Fluid Mech 69:539–563
Malraison B, Atten P (1991) Instabilité électrohydrodynamique due à l'injection d'ions à la surface libre d'un liquid isolant. J Phys III 1:1243–1249
Melcher JR (1963) Field-coupled surface waves. The MIT Press, Cambridge, Mass.
Melcher JR, Schwarz WJ Jr (1968) Interfacial relaxation overstability in a tangential electric field. Phys Fluids 11:2604–2616
Melcher JR, Smith CV Jr (1969) Electrohydrodynamic charge relaxation and interfacial perpendicular-field instability. Phys Fluids 12:778–790
Melcher JR, Taylor GI (1969) Electrohydrodynamics: a review of the role of interfacial shear stresses. Ann Rev Fluid Mech 1:111–146
Néron de Surgy G (1995) Étude des instabilités électrocapillaires. Application aux sources d'ions et d'électrons. These de doctorat, Université de Paris 6
Néron de Surgy G, Chabrerie JP, Denoux O, Wesfreid JE (1993) Linear growth of instabilities on a liquid metal under normal electric field. J Phys II 3:1201–1225
Pérez AT (1997) Rose-window instability in low conducting liquids. J Electrost 40/41:141–146
Pontiga F, Castellanos A (2000) Oscillatory instability in a plane of nonpolar liquid subjected to an electric field. In: 2000 Annual Report of the Conference on Electrical Insulation and Dielectric Phenomena (CEIDP), IEEE Dielect Insulat Soc 97–100
Pontiga F, Castellanos A, Malraison B (1995) Some considerations on the instabilities of nonpolar liquids subjected to charge injection. Phys Fluids 7:1348–1356
Schneider JM, Watson PK (1970) Electrohydrodynamic stability of space-charge-limited currents in dielectric liquids. I. Theoretical study. Phys Fluids 13:1948–1954
Vega F, Pérez AT (1999a) EHD instabilities induced by corona discharge using a triode configuration. In: Proceedings of the Société Française d'Electrostatique, Poitiers. S.F.E., pp 224–228
Vega F, Pérez AT (1999b) Measurements of electric current through a liquid–air interface in corona discharge. In: 1999 Annual Report of the Conference on Electrical Insulation and Dielectric Phenomena (CEIDP). IEEE Dielect Insulat Soc II:818–821
Vega F, Pérez AT (2002) Instability in a non-ohmic/ohmic fluid interface under a perpendicular electric field and unipolar injection. Phys Fluids 14:2738–2751
Watson PK, Clancy TM (1965) Electron injection technique for investigating processes in insulating liquids and solids. Rev Sci Instrum 36:217–222
Watson PK, Schneider JM, Till HR (1970) Electrohydrodynamic stability of space-charge-limited currents in dielectric liquids. II. Phys Fluids 13:1955–1961